

Electromagnetic time reversal algorithms and source localization in lossy dielectric media

Abdul Wahab* Amer Rasheed* Tasawar Hayat^{†‡§} Rab Nawaz *

March 26, 2014

Abstract

The problem of reconstructing the spatial support of an extended radiating electric current source density in a lossy dielectric medium from transient boundary measurements of the tangential components of electric fields is studied. A time reversal algorithm is proposed to localize a source density from loss-less wave-field measurements. Further, in order to recover source densities in a lossy medium, we first build attenuation operators thereby relating loss-less waves with lossy ones. Then based on asymptotic expansions of attenuation operators with respect to attenuation parameter, we propose two time reversal strategies for localization. The losses in electromagnetic wave propagation are incorporated using the Debye's complex permittivity, which is well-adopted for low frequencies (radio and microwave) associated with polarization in dielectrics.

AMS subject classifications. 35L05, 35R30; Secondary 47A52, 65J20

Keywords. Time reversal; Electromagnetic waves; Inverse source problem; Debye's law, Attenuation operators

1 Introduction

Time reversal algorithms have been an important tool to solve inverse problems in science and engineering since their premier applications [1–3]. These algorithms exploit the time invariance and the reciprocity of non-attenuating waves which substantiate that a wave travels through a loss-less medium and converges at the location of its source (scatterer, reflector, or emitter) on re-emission after reversing the time using transformation $t \rightarrow t_{\text{final}} - t$. The idea has been successively used in telecommunication [4–6], biomedical imaging [7], inverse scattering theory [8–10], non-destructive evaluation [11, 12] and prospecting geophysics [13] for instance.

*Department of Mathematics, COMSATS Institute of Information Technology, 47040, Wah Cantt., Pakistan (wahab@ciitwah.edu.pk, amerasheed@ciitwah.edu.pk, rabnawaz@ciitwah.edu.pk).

[†]Department of Mathematics, Quaid-i-Azam University, 45320, Islamabad, Pakistan (pensy_t@yahoo.com).

[‡]Nonlinear Analysis and Applied Mathematics (NAAM) Research Group, Faculty of Science, King Abdulaziz University, Jeddah 21589, Saudi Arabia.

[§]Address correspondence to T. Hayat, E-Mail: pensy_t@yahoo.com

The robustness and simplicity of time-reversal techniques make them an impressive choice to resolve source localization problems. These problems have been the subject of numerous studies over the recent past due to a plethora of applications in diverse domains, especially in biomedical imaging, non destructive testing and geophysics, see for instance [14–24] and references therein. Several frameworks to recover spatial support of the stationary acoustic, elastic and electromagnetic sources in time and frequency domain have been developed [16, 17, 22, 25], including time reversal algorithms [1, 9–11, 14, 15, 20]. The inverse source problems are ill-posed having non-uniqueness issues generally due to the presence of non radiating sources [22, 24, 26]. The stability and localization of radiating electromagnetic sources with single frequency, multiple frequency and complete frequency bandwidth as well as transient data have been studied extensively, refer for instance to [24, 26–30].

An interesting problem in imaging is to model and compensate for the effects of wave attenuation on image quality. Most of the imaging techniques either emphasize a non-attenuating medium or do not adequately incorporate underlying phenomenon in reconstruction algorithms. As a consequence, one retrieves erroneous or less accurate wave synthetics which produce serious blurring in reconstructed images. This is further blended with intrinsic instability and uncertainty of the reconstruction. All together, these effects complicate attempts to track the key features of the image and result in unfortunate information loss, refer to [31] for a detailed account of attenuation artifacts in imaging.

This investigation aims to establish time reversal algorithms for isotropic dielectric lossy media thereby retrieving extended radiating current sources using transient measurements of the tangential components of electric field over an imaging domain in attenuating environment.

Unfortunately, the time-reversibility of waves is forsaken in lossy media thereby impeding classical time reversal algorithms to be applicable. Recently, Ammari et al. [14–19] have extended the time reversal algorithms to attenuating acoustic and elastic media and to inverse source problems using asymptotic expansions of so-called attenuation maps with respect to attenuation parameters. Considering Stoke’s *thermo-viscous wave* model for attenuation two algorithms are implemented in acoustic and elastic media. First an *adjoint wave time reversal* algorithm is established wherein the adjoint lossy wave is re-emitted into the medium. However, since the adjoint lossy wave is explosive in nature, indeed due to the exponentially growing component of the respective adjoint Green functions with frequency, a regularization using frequency truncation of the attenuation maps is discussed. Then, a *pre-processing time reversal* algorithm is established based on a higher order asymptotic development with respect to attenuation parameter by virtue of stationary phase theorem. The asymptotic expansion is utilized to filter the attenuated measurements and subsequently the classical time reversal algorithm is invoked to back propagate the data. Since, the considered attenuation model lacks the *causality* property, the results of these studies were extrapolated to more realistic causal power-law type attenuation models and were combined with variant time reversal strategies by Kalimeris and Scherzer [32] and Kower [33].

In this work, we concentrate on Debye’s complex permittivity model for attenuation and leave the discussion on causality of the model and its generalizations to power-law models for future. Two situations are taken into account. We begin with a non-attenuating medium and afterwards focus on extended source recovery when the medium is lossy and obeys the Debye’s law. We follow the approach by Ammari et al. [15] for constructing imaging functions. In order to achieve time reversal in lossy media, the so-called attenuation maps are identified and their asymptotic developments with respect to Debye’s attenuation parameter

are established informally. The formal developments can still be achieved using theorem of stationary phases or of steepest descent as in [17, 32, 34], and will not be discussed.

The investigation is sorted in the following order. A few preliminary results and some key identities are collected in Section 2. In Section 3, an electromagnetic source is retrieved using transient measurements of the tangential component of electric field in a loss-less medium. Section 4 is dedicated to the construction of attenuation maps. Their asymptotic expansions are derived and lossy time reversal algorithms are established. A few numerical illustrations are provided in Section 5 to elucidate the pertinence of imaging functions proposed in this work. The principle contributions of the investigation are finally summarized in Section 6.

2 Preliminaries

Let $\Omega \subset \mathbb{R}^d$, $d = 2, 3$, be an open bounded domain with a Lipschitz boundary Γ . Consider the time-dependent homogeneous linear Maxwell equations

$$\begin{cases} \nabla \times \mathbf{E}_0(\mathbf{x}, t) + \mu_0 \frac{\partial \mathbf{H}_0}{\partial t}(\mathbf{x}, t) = 0, & (\mathbf{x}, t) \in \mathbb{R}^d \times \mathbb{R}, \\ \nabla \times \mathbf{H}_0(\mathbf{x}, t) - \epsilon_0 \frac{\partial \mathbf{E}_0}{\partial t}(\mathbf{x}, t) = \delta_0(t) \mathbf{J}(\mathbf{x}), & (\mathbf{x}, t) \in \mathbb{R}^d \times \mathbb{R}, \\ \mathbf{E}_0(\mathbf{x}, t) = 0 = \frac{\partial \mathbf{E}_0}{\partial t}(\mathbf{x}, t), & \mathbf{x} \in \mathbb{R}^d, t \ll 0, \\ \mathbf{H}_0(\mathbf{x}, t) = \mathbf{0} = \frac{\partial \mathbf{H}_0}{\partial t}(\mathbf{x}, t), & \mathbf{x} \in \mathbb{R}^d, t \ll 0, \end{cases} \quad (2.1)$$

with electric permittivity $\epsilon_0 > 0$ and permeability $\mu_0 > 0$. \mathbf{E}_0 and \mathbf{H}_0 are the electric and magnetic fields respectively and $\delta_0(t)$ is the Dirac mass at $t = 0$. Here $\mathbf{J}(\mathbf{x}) \in \mathbb{R}^d$ is the radiating current source density. We assume that $\mathbf{J}(\mathbf{x})$ is sufficiently smooth and compactly supported in Ω , that is, $\text{supp}\{\mathbf{J}\} \subset \subset \Omega$.

By virtue of (2.1), fields \mathbf{E}_0 and \mathbf{H}_0 are the solutions to,

$$\begin{cases} \nabla \times \nabla \times \mathbf{E}_0(\mathbf{x}, t) + \frac{1}{c_0^2} \frac{\partial^2}{\partial t^2} \mathbf{E}_0(\mathbf{x}, t) = -\mu_0 \mathbf{J}(\mathbf{x}) \frac{\partial \delta_0(t)}{\partial t}, & (\mathbf{x}, t) \in \mathbb{R}^d \times \mathbb{R}, \\ \mathbf{E}_0(\mathbf{x}, t) = \mathbf{0} = \frac{\partial \mathbf{E}_0}{\partial t}(\mathbf{x}, t), & \mathbf{x} \in \mathbb{R}^d, t \ll 0, \end{cases} \quad (2.2)$$

and

$$\begin{cases} \nabla \times \nabla \times \mathbf{H}_0(\mathbf{x}, t) + \frac{1}{c_0^2} \frac{\partial^2}{\partial t^2} \mathbf{H}_0(\mathbf{x}, t) = \nabla \times \mathbf{J}(\mathbf{x}) \delta_0(t), & (\mathbf{x}, t) \in \mathbb{R}^d \times \mathbb{R}, \\ \mathbf{H}_0(\mathbf{x}, t) = \mathbf{0} = \frac{\partial \mathbf{H}_0}{\partial t}(\mathbf{x}, t), & \mathbf{x} \in \mathbb{R}^d, t \ll 0. \end{cases} \quad (2.3)$$

In the sequel, we refer to $\kappa_0 := \omega \sqrt{\epsilon_0 \mu_0} = \omega / c_0$ as the wave number with $c_0 := 1 / \sqrt{\epsilon_0 \mu_0}$ being the wave speed in dielectrics with frequency pulsation ω . Furthermore, we denote by $\hat{v}(\omega)$ or $\mathcal{F}[v(\cdot)](\omega)$ the Fourier transform of a function $v(t)$ with the conventions

$$\hat{v}(\omega) = \int_{\mathbb{R}} v(t) e^{-i\omega t} dt \quad \text{and} \quad v(t) = \frac{1}{2\pi} \int_{\mathbb{R}} \hat{v}(\omega) e^{i\omega t} d\omega.$$

Let $\widehat{\mathbf{E}}_0$ and $\widehat{\mathbf{H}}_0$ be the time-harmonic electric and magnetic fields, that is,

$$\begin{cases} \nabla \times \widehat{\mathbf{E}}_0 + i\omega\mu_0\widehat{\mathbf{H}}_0 = \mathbf{0}, & \mathbf{x} \in \mathbb{R}^d, \\ \nabla \times \widehat{\mathbf{H}}_0 - i\omega\epsilon_0\widehat{\mathbf{E}}_0 = \mathbf{J}(\mathbf{x}), & \mathbf{x} \in \mathbb{R}^d, \end{cases} \quad (2.4)$$

subject to the Silver-Müller radiation conditions

$$\mathbf{0} = \lim_{|\mathbf{x}| \rightarrow \infty} |\mathbf{x}|^{\frac{d-1}{2}} \begin{cases} \sqrt{\mu_0}\widehat{\mathbf{H}}_0 \times \hat{\mathbf{x}} - \sqrt{\epsilon_0}\widehat{\mathbf{E}}_0, \\ \sqrt{\epsilon_0}\widehat{\mathbf{E}}_0 \times \hat{\mathbf{x}} + \sqrt{\mu_0}\widehat{\mathbf{H}}_0, \end{cases} \quad \text{where } \hat{\mathbf{x}} := \frac{\mathbf{x}}{|\mathbf{x}|}. \quad (2.5)$$

Consequently, the time-harmonic fields $\widehat{\mathbf{E}}_0$ and $\widehat{\mathbf{H}}_0$ then satisfy the Helmholtz equations

$$\begin{cases} \nabla \times \nabla \times \widehat{\mathbf{E}}_0 - \kappa_0^2 \widehat{\mathbf{E}}_0 = -i\omega\mu_0\mathbf{J}(\mathbf{x}), & \mathbf{x} \in \mathbb{R}^d, \\ \nabla \times \nabla \times \widehat{\mathbf{H}}_0 - \kappa_0^2 \widehat{\mathbf{H}}_0 = \nabla \times \mathbf{J}(\mathbf{x}), & \mathbf{x} \in \mathbb{R}^d, \end{cases} \quad (2.6)$$

subject to the outgoing radiation conditions (2.5).

2.1 Electromagnetic fundamental solutions

In order to derive a time reversal algorithms for electromagnetic source imaging and to analyze their localization properties, we recall electromagnetic fundamental solutions and discuss some of their important features and properties.

Let $\widehat{\mathbf{G}}_0^{\text{ee}}(\mathbf{x}, \omega)$ and $\widehat{\mathbf{G}}_0^{\text{me}}(\mathbf{x}, \omega)$ be the outgoing electric-electric and magnetic-electric time-harmonic Green functions for the Maxwell equations in \mathbb{R}^d , that is, for all $\mathbf{x} \in \mathbb{R}^d$

$$\begin{cases} \nabla \times \widehat{\mathbf{G}}_0^{\text{ee}}(\mathbf{x}, \omega) - i\omega\mu_0\widehat{\mathbf{G}}_0^{\text{me}}(\mathbf{x}, \omega) = \mathbf{0}, \\ \nabla \times \widehat{\mathbf{G}}_0^{\text{me}}(\mathbf{x}, \omega) + i\omega\epsilon_0\widehat{\mathbf{G}}_0^{\text{ee}}(\mathbf{x}, \omega) = \mathbf{I}\delta_0(\mathbf{x}), \end{cases} \quad (2.7)$$

where \mathbf{I} is $d \times d$ identity matrix. It is well-known, see for instance [35, 36], that for all $\mathbf{x} \neq \mathbf{0}$

$$\begin{cases} \widehat{\mathbf{G}}_0^{\text{ee}}(\mathbf{x}, \omega) = i\omega\mu_0 \left(\mathbf{I} + \frac{1}{\kappa_0^2} \nabla \nabla \right) \widehat{g}_0(\mathbf{x}, \omega), \\ \widehat{\mathbf{G}}_0^{\text{me}}(\mathbf{x}, \omega) = -\nabla \times \mathbf{I} \widehat{g}_0(\mathbf{x}, \omega), \end{cases} \quad (2.8)$$

where $\widehat{g}_0(\mathbf{x}, \omega)$ is the fundamental solution to the Helmholtz operator $-(\Delta + \kappa_0^2)$ in \mathbb{R}^d , subject to Sommerfeld's outgoing radiation conditions, given by

$$\widehat{g}_0(\mathbf{x}, \omega) = \begin{cases} \frac{i}{4} H_0^{(1)}(\kappa_0 |\mathbf{x}|), & \mathbf{x} \neq \mathbf{0}, \mathbf{x} \in \mathbb{R}^2, \\ \frac{1}{4\pi |\mathbf{x}|} \exp\{i\kappa_0 |\mathbf{x}|\}, & \mathbf{x} \neq \mathbf{0}, \mathbf{x} \in \mathbb{R}^3, \end{cases} \quad (2.9)$$

where $H_0^{(1)}$ is the zeroth order Hankel function of first kind.

Let us define $\mathbf{G}_0^{\text{ee}}(\mathbf{x}, t)$ and $\mathbf{G}_0^{\text{me}}(\mathbf{x}, t)$ for all $\mathbf{x} \in \mathbb{R}^d$, and $\tau, t \in \mathbb{R}$ by

$$\mathbf{G}_0^{\text{ee}}(\mathbf{x}, t) = \mathcal{F}^{-1}[\widehat{\mathbf{G}}_0^{\text{ee}}(\mathbf{x}, \omega)](t) = \frac{1}{2\pi} \int_{\mathbb{R}} \widehat{\mathbf{G}}_0^{\text{ee}}(\mathbf{x}, \omega) e^{i\omega t} d\omega, \quad (2.10)$$

$$\mathbf{G}_0^{\text{me}}(\mathbf{x}, t) = \mathcal{F}^{-1}[\widehat{\mathbf{G}}_0^{\text{me}}(\mathbf{x}, \omega)](t) = \frac{1}{2\pi} \int_{\mathbb{R}} \widehat{\mathbf{G}}_0^{\text{me}}(\mathbf{x}, \omega) e^{i\omega t} d\omega. \quad (2.11)$$

Spatial reciprocity. It can be proved for isotropic dielectrics (see for instance [13]) that for all $\mathbf{x}, \mathbf{y} \in \mathbb{R}^d$, $\mathbf{x} \neq \mathbf{y}$ and $t \in \mathbb{R}$,

$$\mathbf{G}_0^{\text{ee}}(\mathbf{x} - \mathbf{y}, t) = \mathbf{G}_0^{\text{ee}}(\mathbf{y} - \mathbf{x}, t) \quad \text{and} \quad \mathbf{G}_0^{\text{me}}(\mathbf{x} - \mathbf{y}, t) = \mathbf{G}_0^{\text{me}}(\mathbf{y} - \mathbf{x}, t). \quad (2.12)$$

□

The following identities from [37] are the key ingredients to elucidate the localization property of the imaging algorithms proposed in the subsequent sections.

Lemma 2.1 (Electromagnetic Helmholtz-Kirchhoff identity). *Let $\mathbf{B}(0, R)$ be an open ball in \mathbb{R}^d with large radius $R \rightarrow \infty$ and boundary $\partial\mathbf{B}(0, R)$. Then, for all $\mathbf{x}, \mathbf{y} \in \mathbb{R}^d$, we have*

$$\lim_{R \rightarrow +\infty} \int_{\partial\mathbf{B}(0, R)} \widehat{\mathbf{G}}_0^{\text{ee}}(\mathbf{x} - \xi, \omega) \overline{\widehat{\mathbf{G}}_0^{\text{ee}}(\xi - \mathbf{y}, \omega)} d\sigma(\xi) = \mu_0 c_0 \Re \left\{ \widehat{\mathbf{G}}_0^{\text{ee}}(\mathbf{x} - \mathbf{y}, \omega) \right\},$$

where the superposed bar indicates a complex conjugate.

Lemma 2.2. *For all $\mathbf{x}, \mathbf{y} \in \mathbb{R}^d$, $\mathbf{x} \neq \mathbf{y}$,*

$$\frac{\epsilon_0}{2\pi} \int_{\mathbb{R}} \Re \left\{ \widehat{\mathbf{G}}_0^{\text{ee}}(\mathbf{x} - \mathbf{y}, \omega) \right\} d\omega = \delta_{\mathbf{x}}(\mathbf{y}) \mathbf{I}.$$

3 Source reconstruction in ideal media

Assume that we are able to collect the tangential components of the fields \mathbf{E}_0 and \mathbf{H}_0 for all $(\mathbf{x}, t) \in \Gamma \times [0, T]$, for T sufficiently large. If both components on Γ are time-reversed from the final time T (using transformation $t \rightarrow T - t$) and re-emitted from Γ , two fields propagate inside Ω in time reverse chronology converging towards the source $\mathbf{J}(\mathbf{x})$ as $T - t \rightarrow 0$. The ultimate goal of this section is to use the convergence of the back-propagating fields to identify support of the current density $\mathbf{J}(\mathbf{x})$. Precisely, the problem under consideration is the following:

Inverse Source Problem. Given the measurements of the tangential components of the electric and magnetic fields, \mathbf{E}_0 and \mathbf{H}_0 satisfying (2.1), over $\Gamma \times [0, T]$, for T sufficiently large, find the support, $\text{supp}\{\mathbf{J}\}$, of the current source density \mathbf{J} . □

3.1 Time Reversal of the Electric Field

In the rest of this contribution, we concentrate only on the time reversal imaging functions related to the electric field \mathbf{E}_0 in order to identify $\text{supp}\{\mathbf{J}\}$. The case of magnetic field can be dealt with analogously.

Let us introduce an adjoint wave \mathbf{E}_0^s , for a fixed $s \in [0, T]$, satisfying

$$\begin{cases} \nabla \times \nabla \times \mathbf{E}_0^s(\mathbf{x}, t) + \frac{1}{c_0^2} \frac{\partial^2}{\partial t^2} \mathbf{E}_0^s(\mathbf{x}, t) = -\mu_0 \mathbf{d}_e(\mathbf{x}, T - s) \frac{\partial \delta_s(t)}{\partial t} \chi_\Gamma, & (\mathbf{x}, t) \in \mathbb{R}^d \times \mathbb{R}, \\ \mathbf{E}_0^s(\mathbf{x}, t) = \mathbf{0} \quad \text{and} \quad \frac{\partial \mathbf{E}_0^s}{\partial t}(\mathbf{x}, t) = \mathbf{0}, & \mathbf{x} \in \mathbb{R}^d, t \ll s, \end{cases} \quad (3.1)$$

where χ_Γ is the characteristic function of Γ and the data set

$$\mathcal{W}_e = \left\{ \mathbf{d}_e(\mathbf{x}, t) := \nu(\mathbf{x}) \times \mathbf{E}_0(\mathbf{x}, t), \quad \forall (\mathbf{x}, t) \in \Gamma \times [0, T] \right\},$$

contains the tangential component of electric field \mathbf{E}_0 where T is large enough so that electric field and its time derivative almost vanish identically.

By definition, the adjoint wave can be represented for all $(\mathbf{x}, t) \in \mathbb{R}^d \times \mathbb{R}$ as,

$$\mathbf{E}_0^s(\mathbf{x}, t) = - \int_\Gamma \mathbf{G}_0^{\text{ee}}(\mathbf{x} - \xi, t - s) \mathbf{d}_e(\xi, T - s) d\sigma(\xi). \quad (3.2)$$

Each one of these waves is associated with a datum collected at a particular time instance $t = s$ and therefore contributes to the reconstruction of the source on re-emission. In order to gather all the information about source distribution, we add up the adjoint waves \mathbf{E}_0^s for all $s \in [0, T]$. Precisely, we define a time reversal imaging function by

$$\mathcal{J}_0(\mathbf{x}) := \frac{\epsilon_0}{\mu_0 c_0} \int_0^T \mathbf{E}_0^s(\mathbf{x}, T) ds, \quad \mathbf{x} \in \Omega, \quad (3.3)$$

and claim that $\mathcal{J}_0(\mathbf{x}) \simeq \mathbf{J}(\mathbf{x})$. Indeed, we have the following theorem.

Theorem 3.1. *Let \mathcal{J}_0 be the time reversal functional defined by (3.3). For all $\mathbf{x} \in \Omega$ far from the boundary Γ (compared to the wavelength),*

$$\mathcal{J}_0(\mathbf{x}) \simeq \mathbf{J}(\mathbf{x}).$$

Proof. Notice that since \mathbf{J} is compactly supported in Ω , and T is sufficiently large so that the field is negligible outside $[0, T]$,

$$\begin{aligned} \widehat{\mathbf{d}}_e(\xi, \omega) &= \mathcal{F}[\mathbf{d}_e(\xi, \cdot)](\omega) \\ &= \mathcal{F}[\mathbf{E}_0(\xi, \cdot)|_{\Gamma \times [0, T]}](\omega), \\ &\simeq \mathcal{F}[\mathbf{E}_0(\xi, \cdot)|_{\Gamma \times \mathbb{R}}](\omega) \\ &= -\mathcal{F}\left[\int_\Omega \mathbf{G}_0^{\text{ee}}(\mathbf{y} - \xi, \cdot) \mathbf{J}(\mathbf{y}) d\mathbf{y} \Big|_{\Gamma \times \mathbb{R}}\right](\omega), \\ &= -\int_{\mathbb{R}^d} \widehat{\mathbf{G}}_0^{\text{ee}}(\xi - \mathbf{y}, \omega) \mathbf{J}(\mathbf{y}) d\mathbf{y} \Big|_{\xi \in \Gamma}. \end{aligned}$$

Then by using (3.2) in (3.3) and by virtue of Parseval's identity, we have for all $\mathbf{x} \in \Omega$ away from Γ ,

$$\begin{aligned} \mathcal{J}_0(\mathbf{x}) &= -\frac{\epsilon_0}{\mu_0 c_0} \iint_{[0, T] \times \Gamma} \mathbf{G}_0^{\text{ee}}(\mathbf{x} - \xi, t - s) \mathbf{d}_e(\xi, T - s) d\sigma(\xi) ds, \\ &= -\frac{\epsilon_0}{2\pi\mu_0 c_0} \iint_{\mathbb{R} \times \Gamma} \widehat{\mathbf{G}}_0^{\text{ee}}(\mathbf{x} - \xi, \omega) \widehat{\mathbf{d}}_e(\xi, \omega) d\sigma(\xi) d\omega, \\ &\simeq \frac{\epsilon_0}{2\pi\mu_0 c_0} \iiint_{\mathbb{R}^d \times \mathbb{R} \times \Gamma} \widehat{\mathbf{G}}_0^{\text{ee}}(\mathbf{x} - \xi, \omega) \overline{\widehat{\mathbf{G}}_0^{\text{ee}}(\xi - \mathbf{y}, \omega)} \mathbf{J}(\mathbf{y}) d\sigma(\xi) d\omega d\mathbf{y}, \\ &= \frac{\epsilon_0}{2\pi} \iint_{\mathbb{R}^d \times \mathbb{R}} \left(\frac{1}{\mu_0 c_0} \int_\Gamma \widehat{\mathbf{G}}_0^{\text{ee}}(\mathbf{x} - \xi, \omega) \overline{\widehat{\mathbf{G}}_0^{\text{ee}}(\xi - \mathbf{y}, \omega)} d\sigma(\xi) \right) \mathbf{J}(\mathbf{y}) d\omega d\mathbf{y}. \quad (3.4) \end{aligned}$$

Now invoking Lemma 2.1, we obtain

$$\frac{1}{\mu_0 c_0} \int_{\Gamma} \widehat{\mathbf{G}}_0^{\text{ee}}(\mathbf{x} - \xi, \omega) \overline{\widehat{\mathbf{G}}_0^{\text{ee}}(\xi - \mathbf{y}, \omega)} d\sigma(\xi) \simeq \Re \left\{ \widehat{\mathbf{G}}_0^{\text{ee}}(\mathbf{x} - \mathbf{y}, \omega) \right\},$$

and therefore we have

$$\begin{aligned} \mathcal{J}_0(\mathbf{x}) &\simeq \frac{\epsilon_0}{2\pi} \iint_{\mathbb{R}^d \times \mathbb{R}} \Re \left\{ \widehat{\mathbf{G}}_0^{\text{ee}}(\mathbf{x} - \mathbf{y}, \omega) \right\} d\omega \mathbf{J}(\mathbf{y}) d\mathbf{y}, \\ &= \int_{\mathbb{R}^d} \left(\frac{\epsilon_0}{2\pi} \int_{\mathbb{R}} \Re \left\{ \widehat{\mathbf{G}}_0^{\text{ee}}(\mathbf{x} - \mathbf{y}, \omega) \right\} d\omega \right) \mathbf{J}(\mathbf{y}) d\mathbf{y}, \\ &= \int_{\mathbb{R}^d} \delta_{\mathbf{x}}(\mathbf{y}) \mathbf{J}(\mathbf{y}) d\mathbf{y} \\ &= \mathbf{J}(\mathbf{x}), \end{aligned}$$

where we have made use of the identity

$$\frac{\epsilon_0}{2\pi} \int_{\mathbb{R}} \Re \left\{ \widehat{\mathbf{G}}_0^{\text{ee}}(\mathbf{x} - \mathbf{y}, \omega) \right\} d\omega = \delta_{\mathbf{x}}(\mathbf{y}) \mathbf{I},$$

from Lemma 2.2. □

4 Source reconstruction in lossy media

In this section, we present a time reversal strategy for imaging in lossy media. We consider a Debye law to incorporate losses in wave propagation, which is suitable for low frequencies (radio to microwave) associated with polarization in dielectrics [5, 6, 38]. We will only consider the electric case.

Let $\widehat{\mathbf{E}}_a(\mathbf{x}, \omega)$ be the electric field in a lossy dielectric medium, that is, the solution to

$$\nabla \times \nabla \times \widehat{\mathbf{E}}_a(\mathbf{x}, \omega) - (\kappa_a^\sigma(\omega))^2 \widehat{\mathbf{E}}_a(\mathbf{x}, \omega) = -i\omega\mu_0 \mathbf{J}(\mathbf{x}), \quad (\mathbf{x}, \omega) \in \mathbb{R}^d \times \mathbb{R}, \quad (4.1)$$

subject to Sommerfeld radiation condition,

$$\lim_{|\mathbf{x}| \rightarrow \infty} |\mathbf{x}|^{\frac{d-1}{2}} \left| \nu \times \nabla \times \widehat{\mathbf{E}}_a(\mathbf{x}, \omega) - i\kappa_a^\sigma(\omega) \widehat{\mathbf{E}}_a(\mathbf{x}, \omega) \right| = \mathbf{0},$$

where $\kappa_a^\sigma(\omega) = \omega \sqrt{\mu_0 \epsilon_a^\sigma}$ is the wave-number defined in terms of the Debye's complex permittivity:

$$\epsilon_a^\sigma = \epsilon_\infty + \frac{\epsilon_s - \epsilon_\infty}{1 + i a \omega} - \frac{i \sigma}{\omega \epsilon_0}. \quad (4.2)$$

Here ϵ_s , ϵ_∞ , σ and a are respectively, the static and infinite-frequency permittivities, electric conductivity and Debye's loss constant. We precise that $\epsilon_\infty \leq \epsilon_s$. Furthermore, we fix

$$\mathbf{E}_a(\mathbf{x}, t) := \mathcal{F}^{-1}[\widehat{\mathbf{E}}_a(\mathbf{x}, \cdot)](t) = \int_{\mathbb{R}} \widehat{\mathbf{E}}_a(\mathbf{x}, \omega) e^{i\omega t} d\omega.$$

Let $\widehat{\mathbf{G}}_a^{\text{ee}}(\mathbf{x}, \omega)$ be the attenuating electric-electric Green function, *i.e.* the outgoing fundamental solution to the lossy Helmholtz equation

$$\nabla \times \nabla \times \widehat{\mathbf{G}}_a^{\text{ee}}(\mathbf{x}, \omega) - (\kappa_a^\sigma(\omega))^2 \widehat{\mathbf{G}}_a^{\text{ee}}(\mathbf{x}, \omega) = i\omega\mu_0 \delta_0(\mathbf{x}) \mathbf{I}. \quad (4.3)$$

In the sequel, we use the following notation

$$\mathbf{G}_a^{\text{ee}}(\mathbf{x}, t) := \mathcal{F}^{-1} \left[\widehat{\mathbf{G}}_a^{\text{ee}}(\mathbf{x}, \cdot) \right] (t) = \int_{\mathbb{R}} \widehat{\mathbf{G}}_a^{\text{ee}}(\mathbf{x}, \omega) e^{i\omega t} d\omega,$$

and define $\epsilon_{-a}^{-\sigma}$ and $\kappa_{-a}^{-\sigma}$ and the Green functions $\widehat{\mathbf{G}}_{-a}^{\text{ee}}$ and $\mathbf{G}_{-a}^{\text{ee}}$ analogously.

4.1 Attenuation operators

Recall that

$$\nabla \times \nabla \times \widehat{\mathbf{G}}_0^{\text{ee}}(\mathbf{x}, \omega) - \frac{\omega^2}{c_0^2} \widehat{\mathbf{G}}_0^{\text{ee}}(\mathbf{x}, \omega) = i\omega\mu_0\delta_0(\mathbf{x}). \quad (4.4)$$

Therefore, by replacing real frequency ω with $c_0\kappa_a^\sigma(\omega)$ by invoking Theorem of Titchmarsh [39] since $\Im m\{c_0\kappa_a^\sigma(\omega)\} > 0$, using an argument of the unique outgoing fundamental solution and comparing with Equation (4.3), we deduce that

$$\widehat{\mathbf{G}}_0^{\text{ee}}(\mathbf{x}, c_0\kappa_a^\sigma(\omega)) = \frac{c_0\kappa_a^\sigma(\omega)}{\omega} \widehat{\mathbf{G}}_a^{\text{ee}}(\mathbf{x}, \omega), \quad \forall \mathbf{x} \in \mathbb{R}^d, \mathbf{x} \neq \mathbf{0}$$

or equivalently

$$\mathbf{G}_a^{\text{ee}}(\mathbf{x}, t) = \mathcal{L}_a [\mathbf{G}_0^{\text{ee}}(\mathbf{x}, \cdot)] (t).$$

Here we define the operator \mathcal{L}_a (hereafter called attenuation operator) as follows:

$$\begin{aligned} \mathcal{L}_a : \quad \mathbb{S}'([0, \infty)) &\longrightarrow \mathbb{S}'(\mathbb{R}) \\ \phi(t) &\longmapsto \frac{1}{2\pi} \int_{\mathbb{R}} \frac{\omega}{c_0\kappa_a^\sigma(\omega)} \left(\int_{\mathbb{R}^+} \phi(\tau) \exp \{ -ic_0\kappa_a^\sigma(\omega)\tau \} d\tau \right) e^{i\omega t} d\omega, \end{aligned} \quad (4.5)$$

where \mathbb{S} is the Schwartz space of rapidly decreasing functions and \mathbb{S}' is the space of tempered distributions.

Let us also introduce operator $\mathcal{L}_{-a,\rho}$ related to $\kappa_{-a}^{-\sigma}(\omega)$ and its adjoint operator $\mathcal{L}_{-a,\rho}^*$ for all $\rho > 0$ by:

$$\begin{aligned} \mathcal{L}_{-a,\rho} : \quad \mathbb{S}'([0, \infty)) &\longrightarrow \mathbb{S}'(\mathbb{R}) \\ \phi(t) &\longmapsto \frac{1}{2\pi} \int_{\mathbb{R}^+} \phi(\tau) \int_{\omega \leq \rho} \frac{\omega e^{i\omega t}}{c_0\kappa_{-a}^{-\sigma}(\omega)} \exp \{ -ic_0\kappa_{-a}^{-\sigma}(\omega)\tau \} d\omega d\tau, \end{aligned} \quad (4.6)$$

and

$$\begin{aligned} \mathcal{L}_{-a,\rho}^* : \quad \mathbb{S}'([0, \infty)) &\longrightarrow \mathbb{S}'(\mathbb{R}) \\ \phi(t) &\longmapsto \frac{1}{2\pi} \int_{\omega \leq \rho} \frac{\omega}{c_0\kappa_{-a}^{-\sigma}(\omega)} \left(\int_{\mathbb{R}^+} \phi(\tau) e^{i\omega\tau} d\tau \right) \exp \{ -ic_0\kappa_{-a}^{-\sigma}(\omega)t \} d\omega. \end{aligned} \quad (4.7)$$

We extend operators \mathcal{L}_a , $\mathcal{L}_{-a,\rho}$ and $\mathcal{L}_{-a,\rho}^*$ to \mathbf{G}_0^{ee} , that is, for all constant vectors $\mathbf{p} \in \mathbb{R}^d$, we define

$$\mathcal{L}_a[\mathbf{G}_0^{\text{ee}}]\mathbf{p} = \mathcal{L}_a[\mathbf{G}_0^{\text{ee}}\mathbf{p}],$$

$$\mathcal{L}_{-a,\rho}[\mathbf{G}_0^{\text{ee}}]\mathbf{p} = \mathcal{L}_{-a,\rho}[\mathbf{G}_0^{\text{ee}}\mathbf{p}],$$

and

$$\mathcal{L}_{-a,\rho}^*[\mathbf{G}_0^{\text{ee}}]\mathbf{p} = \mathcal{L}_{-a,\rho}^*[\mathbf{G}_0^{\text{ee}}\mathbf{p}].$$

4.2 Asymptotic analysis of attenuation operators

We assume that the attenuation parameter a is sufficiently small compared to the wave-length (denoted by λ), that is,

$$a \ll c_0 \omega^{-1} =: \lambda.$$

For brevity, we consider the case of a non-conductive medium, that is, $\sigma = 0$. Henceforth, we drop the superscript from κ_a^σ and κ_{-a}^σ for simplicity. Then

$$\begin{aligned} c_0 \kappa_a(\omega) &= \frac{\omega}{\sqrt{\epsilon_0}} \sqrt{\epsilon_\infty + \frac{(\epsilon_s - \epsilon_\infty)}{1 + i\omega a}}, \\ &\simeq \frac{\omega}{\sqrt{\epsilon_0}} \sqrt{\epsilon_\infty + (\epsilon_s - \epsilon_\infty) [1 - (i\omega a)] + o(\omega a)}, \\ &\simeq \gamma \omega \sqrt{1 - i\beta \omega a + o(\omega a)}, \\ &\simeq \gamma \omega \left(1 - i\frac{\beta}{2} \omega a \right) + o(\omega a), \end{aligned}$$

and

$$c_0 \kappa_{-a}(\omega) \simeq \gamma \omega \left(1 + i\frac{\beta}{2} \omega a \right) + o(\omega a).$$

where $\beta = (1 - (\epsilon_\infty/\epsilon_s))$ and $\gamma = \sqrt{\epsilon_s/\epsilon_0}$. Similarly, we have

$$\frac{\omega}{c_0 \kappa_a(\omega)} = \frac{1}{\gamma \sqrt{1 - i\beta \omega a + o(\omega a)}} \simeq \frac{1}{\gamma} \left(1 + i\frac{\beta}{2} \omega a \right) + o(\omega a).$$

and

$$\frac{\omega}{c_0 \kappa_{-a}(\omega)} = \frac{1}{\gamma \sqrt{1 + i\beta \omega a + o(\omega a)}} \simeq \frac{1}{\gamma} \left(1 - i\frac{\beta}{2} \omega a \right) + o(\omega a).$$

Then the following result holds.

Lemma 4.1. *Let $\phi \in \mathcal{C}_0^\infty([0, \infty))$, where \mathcal{C}_0^∞ is the space of \mathcal{C}^∞ -functions with compact support in $[0, \infty)$. Then,*

1. *Up to leading order of attenuation parameter a*

$$\mathcal{L}_a[\phi(\cdot)](t) \simeq \frac{1}{\gamma^2} \phi\left(\frac{t}{\gamma}\right) + \frac{\beta a}{2\gamma^3} [\phi' + (t\phi)']\left(\frac{t}{\gamma}\right) \quad \text{as } a \rightarrow 0.$$

2. *For all $\rho > 0$, up to leading order of attenuation parameter a*

$$\mathcal{L}_{-a,\rho}^*[\phi(\cdot)](t) \simeq \frac{1}{\gamma} \mathcal{P}_\rho[\phi(\cdot)](\gamma t) - \frac{\beta a}{2\gamma^2} \mathcal{P}_\rho[\phi' + (t\phi)'](\gamma t) \quad \text{as } a \rightarrow 0.$$

3. *For all $\rho > 0$, up to leading order of attenuation parameter a*

$$\mathcal{L}_{-a,\rho}^*[\mathcal{L}_a[\phi(\cdot)]](t) \simeq \frac{1}{\gamma^3} \mathcal{P}_\rho[\phi(\cdot)](t) + o(a).$$

where \mathcal{P}_ρ is defined by

$$\begin{aligned} \mathcal{P}_\rho : \quad \mathbb{S}'(\mathbb{R}) &\longrightarrow \mathbb{S}'(\mathbb{R}) \\ \phi(t) &\longmapsto \frac{1}{2\pi} \int_{|\omega| \leq \rho} e^{-i\omega t} \mathcal{F}[\phi](\omega) d\omega. \end{aligned} \quad (4.8)$$

Proof. We prove only Statements 1 and 2. Statement 3 is an immediate consequence of Statements 1 and 2.

1. As $a \rightarrow 0$ the attenuation operator \mathcal{L}_a can be approximated by:

$$\begin{aligned} \mathcal{L}_a[\phi](t) &\simeq \frac{1}{2\pi\gamma} \int_{\mathbb{R}} \left(1 + i\frac{\beta}{2}\omega a\right) \left\{ \int_{\mathbb{R}^+} e^{-\gamma\frac{\beta}{2}a\omega^2\tau} \phi(\tau) e^{-i\gamma\omega\tau} d\tau \right\} e^{i\omega t} d\omega + o(a), \\ &\simeq \frac{1}{2\pi\gamma} \int_{\mathbb{R}} \left(1 + i\frac{\beta}{2}\omega a\right) \left\{ \int_{\mathbb{R}^+} \left(1 - \gamma\frac{\beta}{2}a\omega^2\tau\right) \phi(\tau) e^{-i\gamma\omega\tau} d\tau \right\} e^{i\omega t} d\omega + o(a), \\ &\simeq \frac{1}{2\pi\gamma} \iint_{\mathbb{R} \times \mathbb{R}^+} \phi(\tau) e^{-i\gamma\omega\tau} e^{i\omega t} d\tau d\omega \\ &\quad + \frac{\beta a}{2} \frac{1}{2\pi\gamma} \int_{\mathbb{R}} i\omega \int_{\mathbb{R}^+} \phi(\tau) e^{-i\gamma\omega\tau} e^{i\omega t} d\tau d\omega \\ &\quad + \frac{\beta a}{2} \frac{1}{2\pi} \int_{\mathbb{R}} (i\omega)^2 \int_{\mathbb{R}^+} [\tau\phi(\tau)] e^{-i\gamma\omega\tau} e^{i\omega t} d\tau d\omega + o(a), \\ &\simeq \frac{1}{\gamma^2} \phi\left(\frac{t}{\gamma}\right) + \frac{\beta a}{2\gamma^3} [\phi' + (t\phi)']\left(\frac{t}{\gamma}\right) + o(a), \end{aligned}$$

which is the required result.

2. Let the support of ϕ be contained in $[0, t_{\max}] \subsetneq [0, \infty)$. As $a \rightarrow 0$ the operator $\mathcal{L}_{-a,\rho}^*$ can be approximated by:

$$\begin{aligned} \mathcal{L}_{-a,\rho}^*[\phi(\cdot)](t) &\simeq \frac{1}{2\pi\gamma} \int_{|\omega| \leq \rho} \frac{\omega}{c_0\kappa_{-a}(\omega)} \exp\{-ic_0\kappa_{-a}(\omega)t\} \\ &\quad \times \left\{ \int_0^{t_{\max}} \phi(\tau) e^{i\omega\tau} d\tau \right\} d\omega + o(a), \\ &\simeq \frac{1}{2\pi\gamma} \int_{|\omega| \leq \rho} \int_0^{t_{\max}} \left(1 - i\frac{\beta}{2}\omega a\right) \\ &\quad \times \exp\left\{-i\gamma\omega \left(1 + i\frac{\beta}{2}\omega a\right)t\right\} \phi(\tau) e^{i\omega\tau} d\tau d\omega + o(a), \end{aligned}$$

where we have made use of the approximation of lossy wavenumber κ_{-a} for $a \ll c_0\omega^{-1}$.

On further simplifications, we arrive at

$$\begin{aligned}
\mathcal{L}_{-a,\rho}^*[\phi(\cdot)](t) &\simeq \frac{1}{2\pi\gamma} \iint_{[-\rho,\rho] \times [0,t_{\max}]} \left(1 - i\frac{\beta}{2}\omega a\right) e^{\gamma\frac{\beta}{2}\omega^2 at} \\
&\quad \times \phi(\tau) e^{-i\gamma\omega t + i\omega\tau} d\tau d\omega + o(a), \\
&\simeq \frac{1}{2\pi\gamma} \iint_{[-\rho,\rho] \times [0,t_{\max}]} \left(1 - i\frac{\beta}{2}\omega a\right) \left(1 + \gamma\frac{\beta}{2}a\omega^2 t\right) \\
&\quad \times \phi(\tau) e^{-i\gamma\omega t} e^{i\omega\tau} d\tau d\omega + O(a), \\
&\simeq \frac{1}{2\pi\gamma} \iint_{[-\rho,\rho] \times \mathbb{R}^+} \phi(\tau) e^{-i\gamma\omega t} e^{i\omega\tau} d\tau d\omega \\
&\quad - \frac{\beta a}{2} \frac{1}{2\pi\gamma} \int_{|\omega| \leq \rho} i\omega \int_{\mathbb{R}^+} \phi(\tau) e^{-i\gamma\omega t} e^{i\omega\tau} d\tau d\omega \\
&\quad - \frac{\beta a}{2} \frac{1}{2\pi} \int_{|\omega| \leq \rho} (i\omega)^2 \int_{\mathbb{R}^+} [\tau\phi(\tau)] e^{-i\gamma\omega t} e^{i\omega\tau} d\tau d\omega + o(a).
\end{aligned}$$

Finally on introducing the operator \mathcal{P}_ρ , we arrive at

$$\mathcal{L}_{-a,\rho}^*[\phi(\cdot)](t) \simeq \frac{1}{\gamma} \mathcal{P}_\rho[\phi(\cdot)](\gamma t) - \frac{\beta a}{2\gamma^2} \mathcal{P}_\rho[\phi' + (t\phi)'](\gamma t) + o(a).$$

□

Remark 4.2. We precise that the Lemma 4.1, can be proved formally using the argument of stationary phase theorem or steepest decent theorem as in [17, 32, 34].

4.3 Time reversal of the electric field in lossy media

Suppose we are able to collect the tangential components of the attenuated electric field, \mathbf{E}_a , for all $t \in [0, T]$ over Γ , that is we are in possession of the data set

$$\mathcal{W}_{e,a} := \left\{ \mathbf{d}_{e,a}(\mathbf{x}, t) := \nu \times \mathbf{E}_a(\mathbf{x}, t) : (\mathbf{x}, t) \in \Gamma \times [0, T] \right\}.$$

If we simply time-reverse and re-emit the measured data $\mathbf{d}_{e,a}$ in attenuating medium, the electric field is attenuated twice, that is, both in direct and back-propagation. Therefore, resolution of the reconstruction, when localizing the spatial support of the sources, is forsaken. In this section, we present two time reversal strategies for localizing $\text{supp}\{\mathbf{J}\}$ in a lossy medium.

4.3.1 Adjoint operator approach

In order to compensate for losses, we back propagate the measured data using the adjoint wave operator. Unfortunately the adjoint wave problem is severely ill-posed, somewhat similar phenomenon was observed in acoustic and elastic media. Therefore, high frequencies must be suppressed as in the acoustic and elastic cases; refer to [31, Remark 2.3.6]. More precisely, let

$$\mathbf{E}_a^s(\mathbf{x}, t) := \mathcal{F}^{-1} \left[\widehat{\mathbf{E}}_a^s(\mathbf{x}, \cdot) \right](t)$$

be the adjoint (time reversed) field corresponding to datum $\mathbf{d}_{e,a}(\mathbf{x}, t)$ at time $t = s$ propagating inside the medium, where $\widehat{\mathbf{E}}_a^s(\mathbf{x}, \omega)$ is the solution to adjoint lossy Helmholtz equation

$$\left(\nabla \times \nabla \times \widehat{\mathbf{E}}_a^s - \kappa_{-a}^2 \widehat{\mathbf{E}}_a^s \right) (\mathbf{x}, \omega) = -i\omega\mu_0 \overline{\mathbf{d}}_{e,a}(\mathbf{x}, \omega) \chi_\Gamma(\mathbf{x}), \quad (\mathbf{x}, \omega) \in \mathbb{R}^d \times \mathbb{R},$$

and let

$$\mathbf{E}_{a,\rho}^s(\mathbf{x}, t) := \mathcal{P}_\rho [\mathbf{E}_a^s(\mathbf{x}, \cdot)](t),$$

where ρ is the cutoff frequency. Here ρ is chosen in such a way that $\mathbf{E}_{a,\rho}^s$ does not explode whereas the resolution of the time reversal algorithm remains reasonably intact, refer to [31, Remark 2.3.6] for further details. The aim of this section is to justify that $\mathcal{J}_{a,\rho}(\mathbf{x})$ is an approximation of $\mathbf{J}(\mathbf{x})$ up to leading order of Debye's loss parameter a , when $\rho \rightarrow +\infty$, where

$$\mathcal{J}_{a,\rho}(\mathbf{x}) := \frac{\epsilon_0 \gamma^3}{\mu_0 c_0} \int_0^T \mathbf{E}_{a,\rho}^s(\mathbf{x}, T) ds, \quad \forall \mathbf{x} \in \Omega. \quad (4.9)$$

We conclude this subsection with the following key result. It simply states that the adjoint operator approach provides a localization of the $\text{supp}\{\mathbf{J}\}$ with a correction to the attenuation effects up to leading order of the damping parameter a .

Theorem 4.3. *For all $\mathbf{x} \in \Omega$ sufficiently far from $\partial\Omega$, compared to wavelength, the truncated time-reversal imaging functional $\mathcal{J}_{a,\rho}$ satisfies,*

$$\mathcal{J}_{a,\rho}(\mathbf{x}) = \mathcal{J}_{0,\rho}(\mathbf{x}) + O(a),$$

where

$$\mathcal{J}_{0,\rho}(\mathbf{x}) := -\frac{\epsilon_0}{\mu_0 c_0} \iint_{[0,T] \times \Gamma} \mathbf{G}_0^{\text{ee}}(\mathbf{x} - \xi, \tau) \mathcal{P}_\rho [\mathbf{d}_e(\xi, \cdot)](\tau) d\sigma(\xi) d\tau.$$

Moreover,

$$\mathcal{J}_{0,\rho}(\mathbf{x}) \rightarrow \mathbf{J}(\mathbf{x}) \quad \text{as } \rho \rightarrow +\infty.$$

Proof. Notice that

$$\mathbf{G}_{-a,\rho}^{\text{ee}}(\mathbf{x}, t) := \mathcal{P}_\rho [\mathbf{G}_{-a}^{\text{ee}}(\mathbf{x}, \cdot)](t) = \mathcal{L}_{-a,\rho} [\mathbf{G}_0^{\text{ee}}(\mathbf{x}, \cdot)](t). \quad (4.10)$$

By virtue of (4.10), $\mathcal{J}_{a,\rho}(\mathbf{x})$ can be rewritten in the form

$$\mathcal{J}_{a,\rho}(\mathbf{x}) = -\frac{\epsilon_0 \gamma^3}{\mu_0 c_0} \iint_{\Gamma \times [0,T]} \mathbf{G}_0^{\text{ee}}(\mathbf{x} - \xi, s) \mathcal{L}_{-a,\rho}^* [\mathbf{d}_{e,a}(\xi, \cdot)](s) ds d\sigma(\xi).$$

Remark as well that $\mathbf{d}_{e,a}(\mathbf{x}, t) = \mathcal{L}_a [\mathbf{d}_e(\mathbf{x}, \cdot)](t)$, where $\mathbf{d}_e(\mathbf{x}, t)$ represents the ideal data, so that

$$\begin{aligned} \mathcal{J}_{a,\rho}(\mathbf{x}) &= -\frac{\epsilon_0 \gamma^3}{\mu_0 c_0} \iint_{\Gamma \times [0,T]} \mathbf{G}_0^{\text{ee}}(\mathbf{x} - \xi, s) \mathcal{L}_{-a,\rho}^* \left[\mathcal{L}_a [\mathbf{d}_e(\xi, \cdot)] \right](s) ds d\sigma(\xi), \\ &= -\frac{\epsilon_0}{\mu_0 c_0} \iint_{\Gamma \times [0,T]} \mathbf{G}_0^{\text{ee}}(\mathbf{x} - \xi, s) \mathcal{P}_\rho [\mathbf{d}_e(\xi, \cdot)](s) ds d\sigma(\xi) + o(a), \\ &= \mathcal{J}_{0,\rho}(\mathbf{x}) + o(a), \end{aligned}$$

by using Lemma 4.1. Finally, from Theorem 3.1

$$-\frac{\epsilon_0}{\mu_0 c_0} \iint_{\Gamma \times [0,T]} \mathbf{G}_0^{\text{ee}}(\mathbf{x} - \mathbf{y}, s) \mathcal{P}_\rho [\mathbf{d}_e(\xi, \cdot)](s) ds d\sigma(\xi) \xrightarrow{\rho \rightarrow \infty} \mathcal{J}_0(\mathbf{x}) \simeq \mathbf{J}(\mathbf{x}),$$

when \mathbf{x} is far away from the boundary Γ . The conclusion follows immediately. \square

4.3.2 Pre-processing approach

According to Lemma 4.1, for weakly attenuating media up to leading order

$$\mathcal{L}_a[\phi(\cdot)](t) \simeq \frac{1}{\gamma^2} \phi\left(\frac{t}{\gamma}\right) + \frac{\beta a}{2\gamma^3} [\phi' + (t\phi)'']\left(\frac{t}{\gamma}\right). \quad (4.11)$$

Therefore, its first order approximate inverse, $\mathcal{L}_{a,1}^{-1}$, can be given by

$$\mathcal{L}_{a,1}^{-1}[\phi(\cdot)](t) = \frac{1}{\gamma} \phi(\gamma t) - \frac{\beta a}{2\gamma^2} (\phi' + (t\phi)'')(\gamma t). \quad (4.12)$$

In the similar fashion, using higher order asymptotic expansions, k^{th} order approximate inverse $\mathcal{L}_{a,k}^{-1}$ can be constructed. Therefore, a pre-processing approach to time reversal can be described in two steps

1. Filter the measured data in order to compensate for the attenuation effects using $\mathcal{L}_{a,k}^{-1}$.
2. Use classical time reversal (in ideal medium) with filtered data as input.

Algorithm 1 Pre-processing Time Reversal Algorithm: k^{th} Order

Require: $\mathcal{W}_{e,a} = \left\{ \mathbf{d}_{e,a}(x, t) := \mathbf{E}_a(x, t) : \forall (x, t) \in \Gamma \times [0, T] \right\}$, $0 < a \ll c_0 \omega^{-1}$ and $k \geq 1$.

- 1: **procedure** FILTER(Pre-process $\mathbf{d}_{e,a}(x, t)$.)
 return $\mathbf{d}_e(x, t) := \mathcal{L}_{a,k}^{-1}[\mathbf{d}_{e,a}(x, \cdot)](t)$.
- 2: **end procedure**
- 3: **procedure** TIME-REVERSAL(Evaluate $\mathcal{J}_0(x)$.)
 for each $s \in [0, T]$ **do**
 Construct $\mathbf{E}_0^s(x, T)$ for $x \in \Omega$ using $\mathbf{d}_e(x, t)$.
 end for
 Evaluate $\mathcal{J}_0(x) := \int_0^T \mathbf{E}_0^s(x, T) ds$.
 return $\mathcal{J}_0(x)$.
- 8: **end procedure**

return $\mathcal{J}_{a,k} = \mathcal{J}_0(x) + o(a^k)$.

Remark 4.4. *Pre-processing approach has two principle advantages over adjoint approach:*

1. *It allows for higher order correction to attenuation artifacts. Indeed using higher order approximations of the operator \mathcal{L}_a , using stationary phase theorem [34], one can iteratively construct higher order pseudo-inverse $\mathcal{L}_{a,k}^{-1}$. Consequently filtered data using $\mathcal{L}_{a,k}^{-1}$ yield a k^{th} order correction for the attenuation artifacts. In this context, we refer to [15, 17, 32]*
2. *It is much more stable numerically than the adjoint operator approach, as it has been observed for the case of acoustic imaging; refer to [14, 15, 19, 31].*

5 Numerical illustrations

The aim here is to numerically illustrate the appositeness of the algorithms proposed in the previous sections. For brevity, we only consider a two dimensional case. In order to numerically resolve the initial value problem (2.2), we use a *Fourier spectral splitting* approach [40] together with a *perfectly matched layer (PML)* technique [41] to simulate a free outgoing interface blended with the *Strang's splitting* method [42].

We consider a rectangular domain $X = [-l/2, l/2] \times [-l/2, l/2]$ such that $\Omega \subset X$ with periodic boundary conditions. For simplicity, we take $\epsilon_0 = 1 = \epsilon_s$ and $\mu_0 = 1$, and consequently $c_0 = 1 = \gamma$. Furthermore, we choose $\epsilon_\infty = 0.5$ and therefore $\beta = 0.5$. Let $\mathbf{E}_0 = (E_1, E_2)$, $\mathbf{J} = (J_1, J_2)$ and $\mathbf{x} = (x_1, x_2)$. Then the system (2.2) can be rewritten as

$$\begin{cases} \frac{\partial^2 \mathbf{E}_0}{\partial t^2}(\mathbf{x}, t) = -\nabla \times \nabla \times \mathbf{E}_0(\mathbf{x}, t), & (\mathbf{x}, t) \in \mathbb{R}^d \times \mathbb{R}, \\ \mathbf{E}_0(\mathbf{x}, t) = -\mathbf{J}(\mathbf{x}) \quad \text{and} \quad \frac{\partial \mathbf{E}_0}{\partial t}(\mathbf{x}, t) = \mathbf{0}, & \mathbf{x} \in \mathbb{R}^d, t \ll 0. \end{cases} \quad (5.1)$$

Let

$$\mathbf{u} = \begin{pmatrix} E_1 \\ \partial_t E_1 \\ E_2 \\ \partial_t E_2 \end{pmatrix}, \quad \mathbf{V} = \begin{pmatrix} 0 & 1 & 0 & 0 \\ \partial_{x_2}^2 & 0 & 0 & 0 \\ 0 & 0 & 0 & 1 \\ 0 & 0 & \partial_{x_1}^2 & 0 \end{pmatrix} \quad \text{and} \quad \mathbf{W} = \begin{pmatrix} 0 & 0 & 0 & 0 \\ 0 & 0 & -\partial_{x_1} \partial_{x_2} & 0 \\ 0 & 0 & 0 & 0 \\ -\partial_{x_1} \partial_{x_2} & 0 & 0 & 0 \end{pmatrix}.$$

Then the second order differential equation in (5.1) can be converted to a first order differential equation

$$\partial_t \mathbf{u} = (\mathbf{V} + \mathbf{W}) \mathbf{u}.$$

Subsequently, we integrate the above equation using *Strang's splitting method* [42], which is known to be of $o(t^2)$ and is described as

$$\mathbf{u} = \exp \left\{ -t(\mathbf{V} + \mathbf{W}) \right\} = \exp \left\{ -\frac{t}{2} \mathbf{W} \right\} \exp \left\{ -t \mathbf{V} \right\} \exp \left\{ -\frac{t}{2} \mathbf{W} \right\} + o(t^2).$$

Further, \mathbf{V} is computed exactly in the spatial Fourier space. Indeed, the Fourier transform of $\mathbf{u}_{\mathbf{V}}(\mathbf{x}, t) = \mathbf{u}(\mathbf{x})e^{-\mathbf{V}t}$ satisfies

$$\begin{aligned} \widehat{E_{\mathbf{V},1}}(\mathbf{k}, t) &= \cos(|k_2|t) \widehat{E_1}(\mathbf{k}) + t \operatorname{sinc}(|k_2|t) \widehat{\partial_t E_1}(\mathbf{k}), \\ \widehat{\partial_t E_{\mathbf{V},1}}(\mathbf{k}, t) &= \cos(|k_2|t) \widehat{\partial_t E_1}(\mathbf{k}) - |k_2| \sin(|k_2|t) \widehat{E_1}(\mathbf{k}), \\ \widehat{E_{\mathbf{V},2}}(\mathbf{k}, t) &= \cos(|k_1|t) \widehat{E_2}(\mathbf{k}) + t \operatorname{sinc}(|k_1|t) \widehat{\partial_t E_2}(\mathbf{k}), \\ \widehat{\partial_t E_{\mathbf{V},2}}(\mathbf{k}, t) &= \cos(|k_1|t) \widehat{\partial_t E_2}(\mathbf{k}) - |k_1| \sin(|k_1|t) \widehat{E_2}(\mathbf{k}), \end{aligned}$$

where $\mathbf{k} = (k_1, k_2)$ is the spatial frequency and $\operatorname{sinc}(t) = \sin t/t$ is the classical *sinc* function.

Similarly \mathbf{W} can be integrated to yield

$$\mathbf{u}_{\mathbf{W}}(\mathbf{x}, t) = \mathbf{u}(\mathbf{x})e^{-\mathbf{W}t} = \begin{pmatrix} E_1(\mathbf{x}) \\ \partial_t E_1(\mathbf{x}) + t \partial_{x_1} \partial_{x_2} E_2(\mathbf{x}) \\ E_2(\mathbf{x}) \\ \partial_t E_2(\mathbf{x}) + t \partial_{x_1} \partial_{x_2} E_1(\mathbf{x}) \end{pmatrix}.$$

This global algorithm can be proved stable under a standard CFL condition [40]. Same approach is adopted to simulate the lossy electric fields.

Example 1. We choose Ω to be a unit disk centered at origin and place 1024 equi-distributed sensors on its boundary. We computed the tangential components of the electric fields over $(\mathbf{x}, t) \in X \times [0, T]$ with $l = 4$ and $T = 2$ and the space and time discretization steps are taken respectively $\tau = 2^{-13}T$ and $h = 2^{-9}l$. In Figure 1, a current source reconstruction using time reversal function \mathcal{J}_0 is compared to the initial current source density in a lossless dielectric medium. The reconstructions clearly substantiate the accuracy and a high resolution of the time reversal algorithm \mathcal{J}_0 . \square

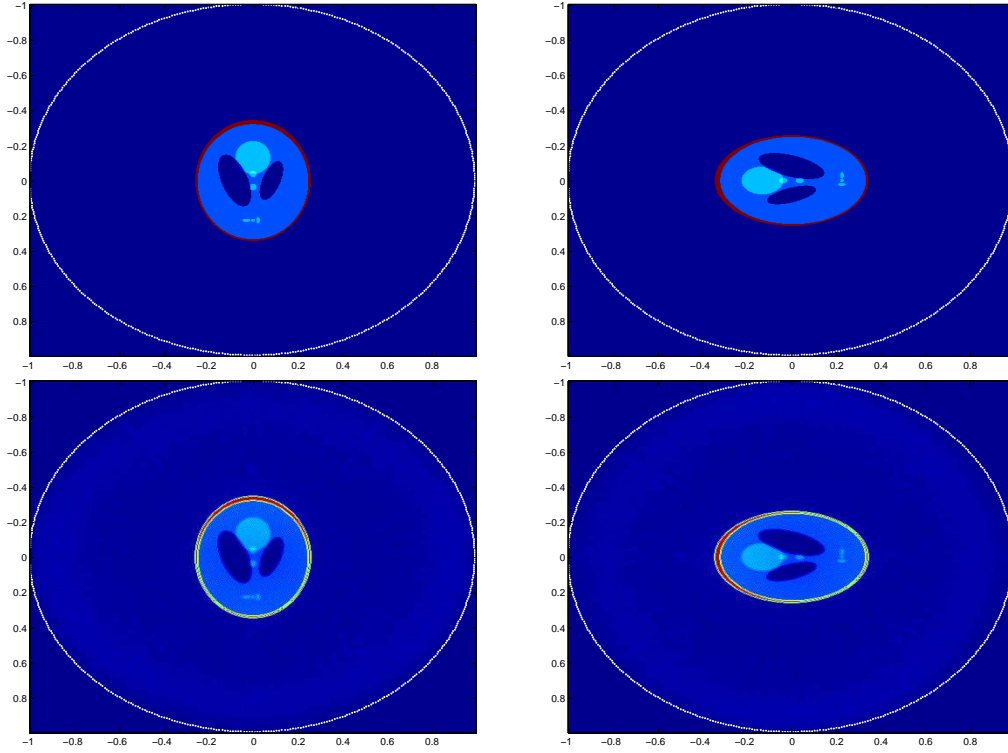


Figure 1: Reconstruction of the initial current source $\mathbf{J} = (J_1, J_2)$ in a non-attenuation medium using time reversal functional \mathcal{J}_0 . Top: Initial source, Bottom: Reconstruction. Left: First component of source density, Right: Second component of source density.

Example 2. Let Ω to be a unit disk centered at origin and place 512 equi-distributed sensors on its boundary. We computed the tangential components of the electric fields over $(\mathbf{x}, t) \in X \times [0, T]$ with $l = 4$ and $T = 2$ and the space and time discretization steps are taken respectively $\tau = 2^{-13}T$ and $h = 2^{-8}l$. Let the Debye's loss parameter a be 2×10^{-4} . The adjoint wave operator approach for time reversal is tested with cut-off frequencies $\rho = 15$ and $\rho = 35$ in Figure 2. The results clearly indicate an improvement in the resolution in successive reconstructions using $\mathcal{J}_{a,\rho}$ as compared to that using \mathcal{J}_0 . The images without

attenuation correction are blurry whereas the edges in images obtained using $\mathcal{J}_{a,\rho}$ are sharper than those obtained using \mathcal{J}_0 and the contrast is relatively higher. \square

Example 3. Let Ω , l , T , τ and h be identical with Example 2 and the Debye's loss parameter a be 4×10^{-4} . In Figure 3, the adjoint wave operator approach for time reversal is tested with cut-off frequencies $\rho = 15$ and $\rho = 25$. Again, the improvement in the contrast and resolution can be remarked. Albeit, as predicted in the previous sections, increasing the cut-off frequency induces numerical instability. To this end, the choice of truncation frequency ρ , of course as a function of attenuation parameter, is very critical. In this regard, we refer to [31, Remark 2.3.6] for a detailed discussion on the issue and for a threshold value of ρ rendering stability while keeping the resolution intact. \square

6 Conclusion

In this investigation, an electromagnetic inverse source problem is tackled using transient boundary measurements of the tangential component of electric field. A time reversal algorithm is established for an extended source localization in non-attenuating media. Motivated by this, two more algorithms based on time reversal framework are proposed in order to deal with the problem associated to lossy media wherein the time reversal invariance breaks down. First an adjoint wave back-propagation technique is proposed and justified using asymptotic expansions versus Debye's attenuation parameter of some ill-conditioned attenuation maps. It is proved that this approach yields the current source density up to leading order of attenuation parameter. Then, a second approach is outlined where the lossy data are pre-processed to yield the ideal (non-attenuating) measurements and subsequently the classical time reversal algorithm is invoked to retrieve the current source density. The numerical illustrations clearly indicate the pertinence of the proposed imaging functions. For brevity, the medium is assumed to be non-conducting, but, the results extend to the case otherwise. Time reversal algorithms for inverse scattering problems in lossy dielectric media can be developed similarly and will be the subject of a fourth coming work.

References

- [1] M. Fink, Time reversed acoustics, *Physics Today*, 50(3):(1997), pp.34.
- [2] L. Borcea, G. C. Papanicolaou, C. Tsogka and J. G. Berryman, Imaging and time reversal in random media, *Inverse Problems*, 18:(2002), pp 12471279.
- [3] J. P. Fouque, J. Garnier, G. Papanicolaou and K. Sølna, *Wave Propagation and Time Reversal in Randomly Layered Media*, Springer, 2007.
- [4] G. Lerosey, J. de Rosny, A. Tourin, A. Derode, G. Montaldo and M. Fink, Time reversal of electromagnetic waves and telecommunication, *Radio Sci.* 40:(2005), RS612.
- [5] M. E. Yavuz and F. L. Teixeira, Full time-domain DORT for ultrawideband electromagnetic fields in dispersive, random inhomogeneous media, *IEEE Transactions on Antennas Propagation*, 54(8):(2006), pp. 2305–2315.

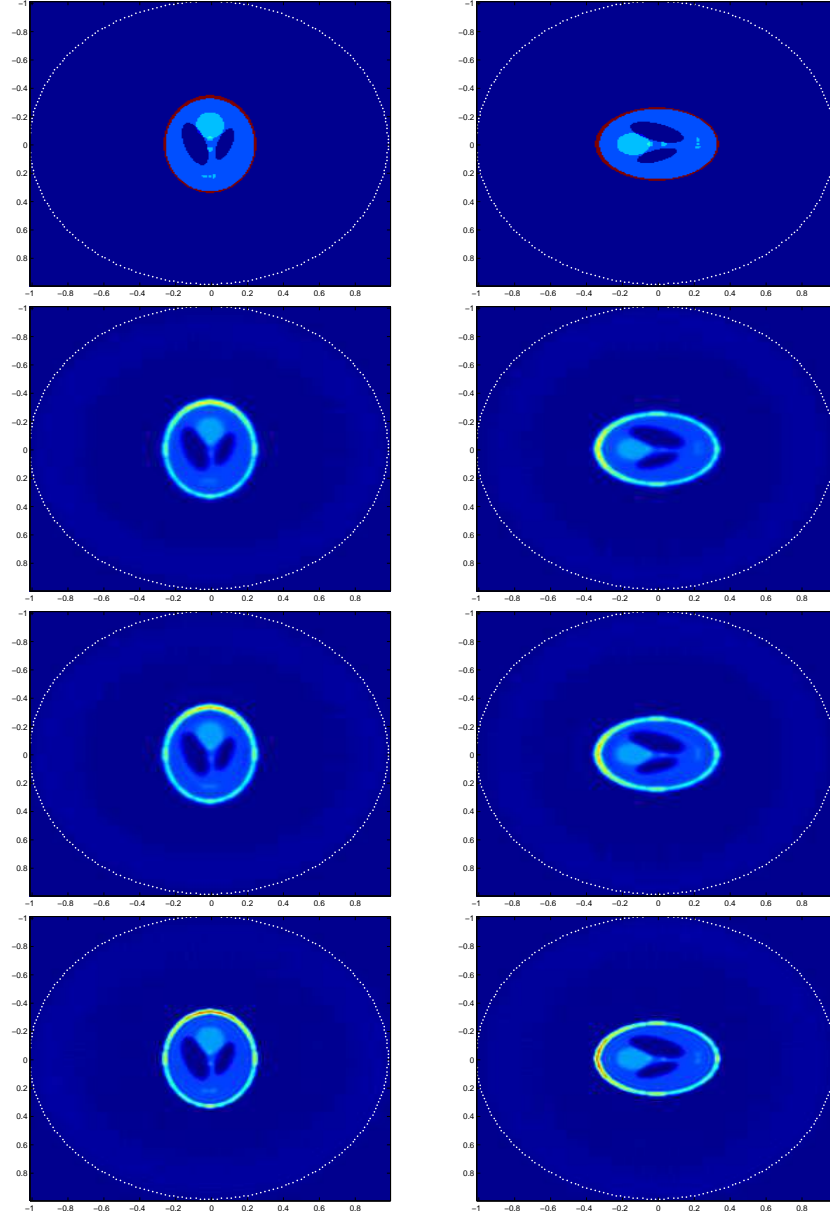


Figure 2: Reconstruction of the spatial support of electric current source $\mathbf{J} = (J_1, J_2)$ in an attenuating medium with $a = 2 \times 10^{-4}$ using time reversal. Left: J_1 , Right: J_2 . Top to bottom: Initial source, reconstruction using \mathcal{J}_0 (without attenuation correction), reconstruction using $\mathcal{J}_{a,\rho}$ with $\rho = 15$ and $\rho = 35$, respectively.

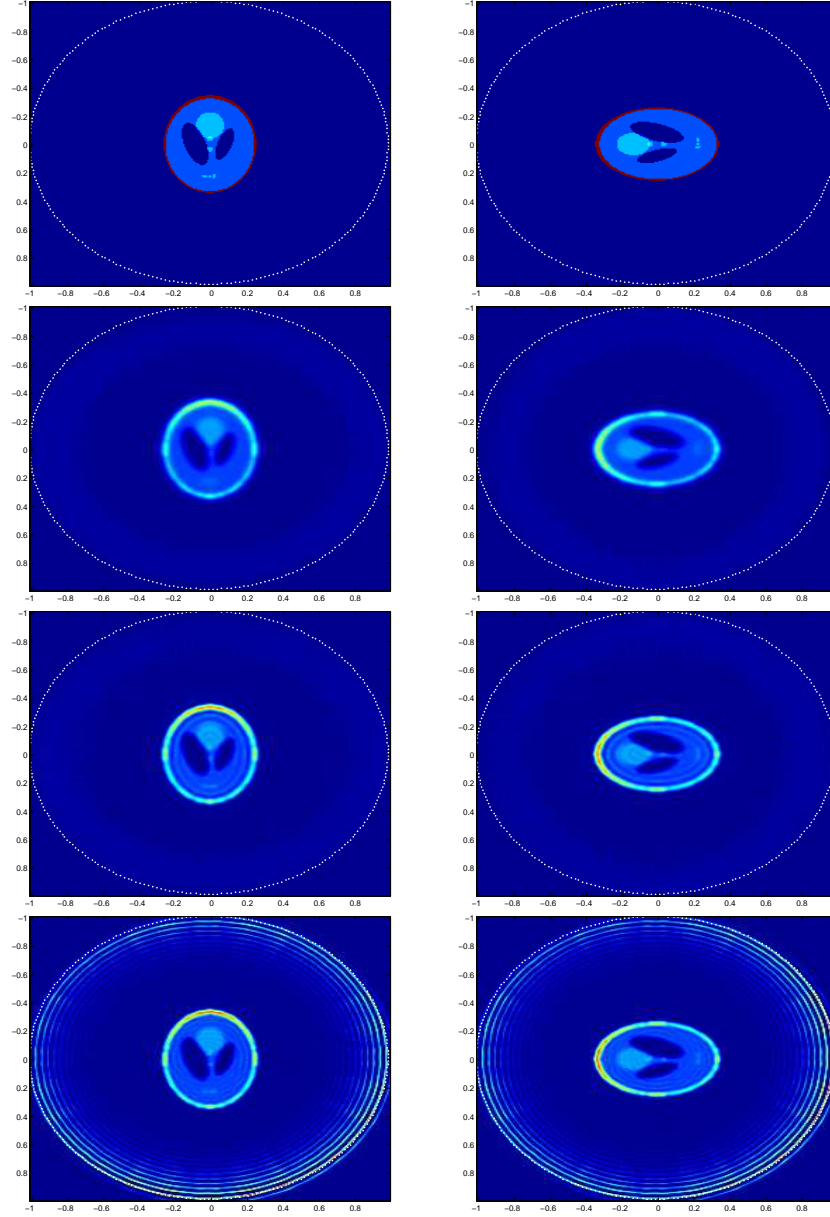


Figure 3: Reconstruction of the spatial support of electric current source density $\mathbf{J} = (J_1, J_2)$ in an attenuating medium with $a = 4 \times 10^{-4}$ using time reversal. Left: J_1 , Right: J_2 . Top to bottom: Initial source, reconstruction using \mathcal{J}_0 (without attenuation correction), reconstruction using $\mathcal{J}_{a,\rho}$ with $\rho = 15$ and $\rho = 25$, respectively.

- [6] M. E. Yavuz and F. L. Teixeira, On the sensitivity of time-reversal imaging techniques to model perturbations, *IEEE Transactions on Antennas Propagation*, 56(3):(2008), pp. 834–842.
- [7] M. Tanter and M. Fink, Time reversing waves for biomedical applications, In *Mathematical Modeling in Biomedical Imaging I*, Lecture Notes in Mathematics, vol. 1983, pp 73–97, Springer-Verlag, Berlin, 2009.
- [8] Y. Xu and L. V. Wang, Time reversal and its application to tomography with diffraction sources, *Physical Review Letters*, 92(3):(2004), 033902.
- [9] S. Gdoura and L. Guadarrama-Bustos, Transient wave imaging of anomalies: a numerical study, in *Mathematical and Statistical Methods for Imaging*, Contemporary Mathematics, vol 548, pp. 31-43, AMS, 2011.
- [10] S. Gdoura, A. Wahab and D. Lesselier, Electromagnetic time reversal and scattering by a small dielectric inclusion, *Journal of Physics: Conference Series*, vol 386: (2012), Paper ID. 012010.
- [11] R. Carminati, R. Pierrat, J. de Rosny and M. Fink, Theory of the time reversal cavity for electromagnetic fields, *Optics Letters*, 32(21):(2007), pp. 3107-3109.
- [12] D. Cassereau and M. Fink, Time-reversal of ultrasonic fields. III. Theory of the closed time-reversal cavity, *IEEE Trans. Ultrasonics, Ferroelect. Freq. Control*, 39(5):(1992), pp. 579-592.
- [13] K. Wapenaar, General representations for wavefields modeling and inversion in geophysics. *Geophysics*, 75(5):(2007), pp. SM5-SM17.
- [14] H. Ammari, E. Bretin, J. Garnier and A. Wahab, Time reversal algorithms in viscoelastic media, *European Journal of Applied Mathematics*, 24(4): (2013), pp 565-600.
- [15] H. Ammari, E. Bretin, J. Garnier and A. Wahab, Time reversal in attenuating acoustic media, in *Mathematical and Statistical Methods for Imaging*, Contemporary Mathematics, vol. 548, pp. 151-163, AMS, 2011.
- [16] H. Ammari, E. Bretin, J. Garnier and A. Wahab, Noise source localization in an attenuating medium, *SIAM Journal on Applied Mathematics*, 72(1): (2012), 317–336.
- [17] H. Ammari, E. Bretin, V. Jugnon and A. Wahab, Photoacoustic imaging for attenuating acoustic media, in *Mathematical Modeling in Biomedical Imaging II*, Lecture Notes Math., vol. 2035, pp. 57-84, Springer, 2012.
- [18] H. Ammari, E. Bretin, J. Garnier, H. Kang, H. Lee, and A. Wahab, *Mathematical Methods in Elasticity Imaging*, submitted.
- [19] H. Ammari, J. Garnier, W. Jing, H. Kang, M. Lim, K. Solna, and H. Wang, *Mathematical and Statistical Methods for Multistatic Imaging*, Lecture Notes in Mathematics, Vol. 2098, Springer, 2014.
- [20] H. Ammari, L. Guadarrama Bustos, P. Garapon and H. Kang, Transient anomaly imaging by the acoustic radiation force, *Journal of Differential Equations*, 249:(2010), pp. 1579–1595.

- [21] H. Ammari, Introduction to Mathematics of Emerging Biomedical Imaging, *Math. & App.*, Vol. 62, Springer, 2008.
- [22] N. P. Valdivia, Electromagnetic source identification using multiple frequency information, *Inverse Problems*, 28:(2012), Article ID 115002.
- [23] C. M. Michel, M. M. Murray, G. Lantz, S. Gonzalez, L. Spinelli and R. Grave de Peralta, EEG source imaging, *Clinical Neurophysiology*, 115:(2004), pp. 2195–2222.
- [24] R. P. Porter and A. J. Devaney, Holography and the inverse source problem, *Journal of Optical Society of America*. 72, pp. 327–330, 1982.
- [25] A Lakhal and A K Louis, Locating radiating sources for Maxwells equations using the approximate inverse, *Inverse Problems*, 24:(2008), Paper ID. 045020.
- [26] N. Bleistein and J. Cohen, Nonuniqueness in the inverse source problem in acoustics and electromagnetics, *Journal of Mathematical Physics*, 18:(1977), 194–201.
- [27] R. Albanese and P. B. Monk, The inverse source problem for Maxwell’s equations, *Inverse Problems* 22(3): (2006), Paper ID. 1023.
- [28] G. Bao, J. Lin and F. Triki, A multi-frequency inverse source problem, *Journal of Differential Equations*, 249(12):(2010), pp. 3443–3465.
- [29] N. N. Bojarski, A survey of the near-field far-field inverse scattering inverse source integral equation, *IEEE Transactions on Antenna and Propagation*, 30(5):(1982), 975–979.
- [30] D. Givoli, E. Turkel, Time reversal with partial information for wave refocusing and scatterer identification, *Comput. Methods Appl. Mech. Engrg.*, 213–216: (2012), pp. 223–242.
- [31] A. Wahab, *Modeling and Imaging of Attenuation in Biological Media*, PhD Thesis, Centre de Mathématiques Appliquées, École Polytechnique, France, 2011.
- [32] K. Kalimeris and O. Scherzer, Photoacoustic imaging in attenuating acoustic media based on strongly causal models, *Mathematical Methods in the Applied Sciences*, 36(16):(2013), pp. 2254–2264.
- [33] R. Kower, On Time Reversal in Photoacoustic Tomography for Tissue Similar to Water, *SIAM Journal on Imaging Sciences*, 7(1):(2014), pp. 509–527.
- [34] L. Hormander, *The Analysis of the Linear Partial Differential Operators I: Distribution Theory and Fourier Analysis*, Classics in Mathematics, Springer-Verlag, Berlin, 2003.
- [35] T. B. Hansen and A. D. Yaghjian, *Plane-Wave Theory of Time-Domain Fields: Near-Field Scanning Applications*, IEEE Press, 1999.
- [36] J. C. Nedelec, *Acoustic and Electromagnetic Equations: Integral Representations for Harmonic Problems*, Applied Mathematical Sciences, Vol. 144, Springer Verlag, 2001.
- [37] A. Wahab, A. Rasheed, R. Nawaz, S. Anjum, Electromagnetic source localization with finite set of frequency measurements, arXiv:1403.5184 [math-ph], 2014.

- [38] M. Y. Koledintseva, K. N. Rozanova, A. Orlandi and J. L. Drewniak, Extraction of Lorentzian and Debye parameters for dielectric and magnetic dispersive materials for FDTD modeling, *Journal of Electrical Engineering*, 153(9/S):(2002), pp. 97-100.
- [39] E. C. Titchmarsh, *Introduction to the Theory of Fourier Integrals*, Clarendon Press, Oxford, 1948.
- [40] C. Canuto, M. Y. Hussaini, A. Quarteroni, and T. A. Zang, *Spectral Methods in Fluid Dynamics*, Springer-Verlag, New York-Heidelberg-Berlin, 1987.
- [41] F. Hastings, J. B. Schneider, and S. L. Broschat, Application of the perfectly matched layer (PML) absorbing boundary condition to elastic wave propagation, *Journal of Acoustical Society of America*, 100:(1996), pp 3061–3069.
- [42] G. Strang, On the construction and comparison of difference schemes, *SIAM Journal on Numerical Analysis*, 5:(1968), pp 506–517.